0026-895X/03/6402-502–511$7.00
MOLECULAR PHARMACOLOGY
Vol. 64, No. 2
2326/1083430
Mol Pharmacol 64:502–511, 2003
Printed in U.S.A.

Prevalence of Necrosis in C_2-Ceramide–Induced Cytotoxicity in NB16 Neuroblastoma Cells

BELÉN RAMOS, JILL M. LAHTI, ENRIQUE CLARO, and SUZANNE JACKOWSKI

Departamento de Fisiología, Universidad de Extremadura, Cáceres, Spain (B.R.); Departments of Infectious Diseases (S.J.) and Genetics and Tumor Cell Biology (J.M.L.), St. Jude Children's Research Hospital, Memphis, Tennessee; and Institut de Neurociències and Departament de Bioquímica i Biología Molecular, Universitat Autònoma de Barcelona, Barcelona, Spain (E.C.).

Received December 9, 2002; accepted May 13, 2003

This article is available online at http://molpharm.aspetjournals.org

ABSTRACT

The mechanism of cell death triggered by C_2-ceramide was investigated using the NB16 neuroblastoma cell line. Treatment of NB16 cells with 20 μM C_2-ceramide for 20 h resulted in approximately 75% loss of cell viability, but only 25% of cells were scored as apoptotic based on terminal deoxynucleotidyl transferase nick-end labeling. Ultrastructural analysis revealed early development of necrotic cytoplasmic vacuolization. After 20 h of treatment with C_2-ceramide, the majority of cells possessed necrotic morphology with pronounced cytoplasmic vacuolization and without any nuclear changes, although a quarter of the cell population also exhibited clear perinuclear chromatin condensation characteristic of apoptosis. Flow cytometric analysis of cells labeled with both annexin V and propidium iodide showed the rapid accumulation of C_2-ceramide–treated cells in the necrotic/late apoptotic fraction. In contrast, cells treated with tumor necrosis factor α plus cycloheximide (TNFα + CHX) first appeared in the early apoptotic fraction and then accumulated in the necrotic/late apoptotic fraction. Both C_2-ceramide and TNFα + CHX increased caspase 8- and 3-like activities in cytosolic extracts; however, treatment of cells with the broad-spectrum caspase inhibitor *N*-benzyloxycarbonyl-Val-Ala-Asp-fluoromethylketone protected NB16 cells from TNFα + CHX-induced cell death but did not prevent C_2-ceramide cytotoxicity. Although C_2-ceramide triggered apoptosis in a fraction of the cells, cell death in the population was primarily caused by necrosis. Thus, C_2-ceramide does not faithfully mimic the effects of apoptotic ligands such as TNFα, which are thought to be mediated by an accumulation of endogenous ceramide. The inhibition of phosphatidylcholine synthesis is a target for C_2-ceramide–mediated cytotoxicity, and this work suggests that other agents that kill cells by inhibiting this pathway may also use a mixture of mechanisms, including necrosis as well as apoptosis.

Cell death takes place through two possible mechanisms: necrosis or apoptosis. Chromatin condensation, cell shrinkage, and the appearance of apoptotic bodies are distinctive traits of apoptosis, whereas necrotic cell death is typically characterized by cytoplasmic vesiculation, cell swelling, and disturbance of cell membrane permeability (Kerr et al., 1972). Apoptosis is a tightly regulated process, unlike necrosis, and recent studies in neuronal excitotoxicity suggest the existence of a "twilight zone" between these two types of cell death (Lipton and Nicotera, 1998). Certain pathological conditions, such as some neurodegenerative diseases (Dal Canto and Gurney, 1994) and ischemia (Majno and Joris, 1995), involve neuronal cell death that does not fit either a typical pattern of apoptosis or necrosis. This nonapoptotic cell death is also a programmed process known as paraptosis (Clarke, 1990; Sperandio et al., 2000), which is characterized mainly by cytoplasmic vacuolization without prominent chromatin condensation and can be caspase-independent (Leist and Jäättelä, 2001).

The sphingolipid ceramide is an intracellular second messenger of stress signals initiated by certain cytokines, radiations, or chemicals, which eventually may trigger apoptosis (Hannun, 1996; Mathias et al., 1998). Ceramide generated by stress is commonly the product of sphingomyelinase (Hannun, 1996; Mathias et al., 1998), although it seems that certain chemicals may increase cellular ceramide and therefore trigger apoptosis by enhancing de novo synthesis via ceramide synthase (Bose et al., 1995). Sphingomyelinase activation by receptors belonging to the tumor necrosis factor (TNF) superfamily has been investigated in detail (Ashkenazi and Dixit, 1998) and depends on the previous activation of initiator caspase 8 by signaling complexes including

This work was supported by National Institutes of Heath grants GM45737 (to S.J.), CA67938 (to J.M.L.), CA72572 (to J.M.L.), Cancer Center CORE support grant CA21765, Spanish Grant BFI 2001-2017 (E.C.) and the American Lebanese Syrian Associated Charities. B.R. is the recipient of a predoctoral fellowship from the Spanish Ministry of Science and Technology.

ABBREVIATIONS: TNF, tumor necrosis factor; PtdCho, phosphatidylcholine; CHX, cycloheximide; PBS, phosphate-buffered saline; C_2-ceramide, *N*-acetyl-D-erythro-sphingosine; z-VAD-fmk, *N*-benzyloxycarbonyl-Val-Ala-Asp-fluoromethylketone; FITC, fluorescein isothiocyanate; DMSO, dimethyl sulfoxide; SJCRH, St. Jude Children's Research Hospital; TUNEL, terminal deoxynucleotidyl transferase dUTP nick-end labeling; PtdSer, phosphatidylserine; PI, propidium iodide; ET-18-OCH_3, 1-*O*-octadecyl-2-*O*-methyl-rac-glycero-3-phosphocholine.

the death domain (Dal Canto and Gurney, 1994; Hannun, 1996; Genestier et al., 1998; Rodriguez-Lafrasse et al., 2002). In contrast, the mechanism of ceramide generation in response to stress signals other than those mediated by death domain-containing receptors (i.e., radiation, oxidative stress) is not as well understood (Mathias et al., 1998). Whatever the detailed mechanism by which ceramide is generated, evidence supporting a signaling role for ceramide in apoptosis has been obtained from the use of more polar, N-linked short-chain analogs like C_2-ceramide and *N*-hexanoyl-D-*erythro*-sphingosine. These molecules, when added exogenously, are thought to mimic the biological effects of some cytokines and environmental stress signals (Hannun and Luberto, 2000). However, short-chain ceramides inhibit the synthesis of PtdCho in several cell types (Allan, 2000; Ramos et al., 2000, 2002). This inhibitory effect is not shared by the more natural, long-chain ceramides (Ramos et al., 2002), and is reminiscent of certain antineoplastic compounds such as ET-18-OCH_3, hexadecylphosphocholine, farnesol, geranylgeraniol, or chelerythrine (Voziyan et al., 1993; Haug et al., 1994; Boggs et al., 1995a,b; Baburina and Jackowski, 1998; Miquel et al., 1998; Anthony et al., 1999). These observations led us to propose that disturbance of PtdCho homeostasis could be the primary target of C_2-ceramide and could account for its cytotoxicity (Ramos et al., 2002).

Given that the molecular basis for C_2-ceramide cytotoxicity may be different from that of endogenous ceramide, we have undertaken the present study to compare the induction of cell death in NB16 neuroblastoma cells by TNFα and C_2-ceramide. This neuroblastoma cell line was selected because it contained functional caspase 8, normal levels of *N*-myc, wild-type p53, and intact apoptotic mechanisms induced by TNFα plus cycloheximide (TNFα + CHX) (Teitz et al., 2000, 2002; J. M. Lahti, T. Teitz, and J. J. Kidd, unpublished results). We show that most C_2-ceramide–treated cells do not display morphological and biochemical traits of apoptosis. Furthermore, even though C_2-ceramide stimulates caspases 8 and 3, these activities are not determinants for the cytotoxic effects of C_2-ceramide, in contrast to the caspase-dependent cytotoxicity of TNFα.

Materials and Methods

Materials. Culture medium developed by Roswell Park Memorial Institute (RPMI 1640 medium) was purchased from Cambrex Bio Science Walkersville, Inc. (Walkersville, MD). Trypan blue, trypsin, phosphate-buffered saline (PBS), glutamine, and penicillin-streptomycin were purchased from Invitrogen (Carlsbad, CA). Fetal bovine serum was from Atlanta Biologicals (Norcross, GA). *N*-Acetyl-D-*erythro*-sphingosine (C_2-ceramide), CHX, and *N*-benzylcarboxycarbonyl-Val-Ala-Asp-fluoromethylketone (z-VAD-fmk) were obtained from Calbiochem-Novabiochem (San Diego, CA). Recombinant human TNFα was obtained from Promega (Madison, WI). ApoAlert Caspase colorimetric assay kit was supplied by BD Biosciences Clontech (Palo Alto, CA). In situ cell death detection kit and Annexin V conjugated to FITC were purchased from Roche Applied Science (Basel, Switzerland). [*methyl*-^{3}H]Choline chloride (80 μCi/mmol) and cytidine diphospho-[*methyl*-^{14}C]choline (55 mCi/mmol) were purchased from American Radiolabeled Chemicals (St. Louis, MO). Phospho-[*methyl*-^{14}C]choline (58 mCi/mmol) was purchased from Amersham Biosciences (Piscataway, NJ). Silica gel thin-layer chromatography plates were supplied by Analtech (Newark, DE). All other chemicals were reagent grade or better.

Cell Culture. Cells were grown in RPMI 1640 medium supplemented with 10% fetal bovine serum, 2 mM glutamine, 50 units/ml penicillin, and 50 μg/ml streptomycin and maintained in a humidified atmosphere of 5% CO_2/95% air at 37°C. Before treatment, cells were trypsinized, counted, and seeded in complete RPMI 1640 medium supplemented with 0.5% (v/v) serum and incubated for at least 2 h to allow cells to attach. After attachment, C_2-ceramide in dimethyl sulfoxide (DMSO) or TNFα plus CHX were added at the indicated concentrations. When present, caspase inhibitor (z-VAD-fmk) was added in ethanol 1 h before the addition of C_2-ceramide or TNFα plus CHX. Ethanol or DMSO alone were added to control cells, so that the final concentration of either vehicle was 0.2% in control and treated cultures. After incubation for the indicated times, adherent and floating cells were collected for analysis.

Viability Determinations. Cells were seeded at a density of 6.12×10^5 in 35-mm dishes and after attachment, the reagents were added to the cultures. Floating and adherent cells were harvested after 18 h, washed with PBS, exposed to 0.2% (w/v) trypan blue dye and counted in a hemocytometer. Four different fields of at least 100 cells each were counted for each determination. Viability was calculated as the percentage of cells that excluded dye relative to the total number.

Electron Microscopy. Cells were seeded at 1.75×10^6 cells in RPMI 1640 medium containing 0.5% serum in 60-mm culture dishes and allowed to attach for at least 2 h. Cells were then incubated 2 to 24 h with 20 or 40 μM C_2-ceramide. Cells were rinsed with PBS and fixed with 2% (v/v) glutaraldehyde in PBS. After fixation, cells were scraped and pelleted by centrifugation. Cell pellets were postfixed with a solution containing 1% (v/v) osmic acid in PBS and stained with 2% uranyl acetate in ethanol. Pellets were dehydrated in graded ethanol (50 to 100%) and embedded in Spurr's resin. Thin sections were poststained with uranyl acetate and Reynolds lead citrate. Samples were examined with a 1200 Ex microscope (JEOL, Tokyo, Japan). Fixation, embedding, and transmission electron microscopy was performed by Dr. K. Gopal Murti (SJCRH Scientific Imaging Shared Resource).

Quantitation of Apoptosis by TUNEL. Apoptotic cells were detected by terminal deoxynucleotidyl transferase nick-end labeling (TUNEL) as described previously (El Mouedden et al., 2000). Trypsinized and floating cells were centrifuged and pelleted cells were rapidly rinsed with PBS containing 1% bovine serum albumin and fixed in 4% formaldehyde for 1 h. After centrifugation and rinsing with PBS, cells were transferred to 96-well plates and treated with 0.3% H_2O_2 in methanol for 10 min to quench endogenous peroxidase activity. Apoptotic cells were detected by terminal deoxynucleotidyl transferase-mediated extension of 3′-OH ends of fragmented DNA, using fluorescein-labeled dUTP as a precursor, according to the instructions from the supplier. DNA-bound fluorescein was detected by reaction with anti-fluorescein antibody conjugated to peroxidase. Peroxidase activity in immunocomplexes was visualized by reaction of diaminobenzidine in H_2O_2. Cells were resuspended in PBS, spread on polylysine-coated slides, and allowed to air dry. Cells were then counterstained with methyl green, rinsed with distilled water, and the preparations were mounted using permanent medium. Enumeration of apoptotic nuclei was made on slides from each experiment, using an E600 Nikon light microscope (Nikon, Tokyo, Japan) with a 50× objective and a 10× eyepiece. We counted all nuclei exhibiting a frank brown labeling as apoptotic. These nuclei most often displayed typical alteration such as pyknosis, crescent-like condensation of chromatin, or segregation into apoptotic bodies. The incidence of apoptotic nuclei was given as the percentage relative to total nuclei. At least 100 cells were counted for each determination.

Caspase Activity. Cells were seeded at a density of 1.75×10^6 in 60-mm dishes and maintained in complete medium plus 0.5% serum for 2 h. When appropriate, cells were preincubated with z-VAD-fmk for 1 h, and then exposed to C_2-ceramide or TNFα + CHX at 0 h. At the indicated times thereafter, the medium was centrifuged to collect

floating cells that were combined with adherent cells that had been washed twice with PBS and scraped from the dishes. The pool of adherent plus nonadherent cells from each time point were then pelleted together and resuspended in 1 ml of cold PBS at 4°C. Caspase activity was measured in cell lysates following the manufacturer's instructions in the ApoAlert caspase kit, using IETD-*para*-nitroaniline to signal caspase-8 and DEVD-*para*-nitroaniline to measure caspase-3.

Flow-Cytometric Analysis of Annexin V and Propidium Iodide-Stained Cells. Cells were seeded at a density of 4.9×10^5 in 35-mm dishes in complete medium and incubated for 24 h. After 24 h, the medium was replaced with medium containing 0.5% serum, and the reagents were added to the cultures. Trypsinized and floating cells were collected after the indicated times. Annexin-V-FITC staining was carried out as described by the manufacturer (Roche Molecular Biochemicals, Mannheim, Germany). Briefly, 3×10^5 cells were washed in PBS and resuspended in 120 μl of binding buffer (10 mM HEPES, pH 7.4, 140 mM NaCl, and 2.5 mM CaCl) containing 2 μl of Annexin-V-FITC and 20 μg/ml propidium iodide (PI). The samples were incubated for 15 min in darkness and 500 μl of binding buffer was added. Cells were filtered through a 40-μm mesh. Cells were analyzed for the presence of apoptotic cells using fluorescence-activated cell sorting analysis as performed by Dr. Richard Ashmun (SJCRH Flow Cytometry Shared Resource).

Metabolic Labeling of Cells. Cells were seeded at a density of 1.4×10^6 cells in 60-mm dishes in complete medium and incubated for 24 h. The medium was replaced with medium containing 0.5% serum and [*methyl*-^{3}H]choline was added as indicated in the legend 2 h before the addition of C_2-ceramide at the indicated final concentrations. At the indicated times, the medium was removed and cells were washed twice with ice-cold PBS. Cells were harvested on ice, washed twice with 1 ml of ice-cold PBS, and then pelleted for extraction of lipids (Bligh and Dyer, 1959). Briefly, the pellet was resuspended in 0.1 ml of water, and 0.24 ml of methanol and 0.15 ml of chloroform were added. After 10 min at room temperature, 0.15 ml of chloroform and 0.12 ml of water were added. The tubes were shaken vigorously and then centrifuged to clearly separate the two phases. The radiolabeled lipid in the lower phase was >95% PtdCho as determined by thin-layer chromatography on Silica Gel G plates developed in chloroform/acetic acid/methanol/water (5:2:4:1). Total radioactivity in the upper aqueous and lower organic phases was quantified by scintillation counting. To separate the water-soluble [^{3}H]choline metabolites, 0.2-ml aliquots of the upper phase were evaporated, resuspended in 40 μl of water, and spotted onto preadsorbent Silica Gel G thin-layer chromatography plates, which were developed in 95% ethanol/2% NH_4OH (1:1, v/v). Identification of radiolabeled choline, phosphocholine, and cytidine diphosphocholine was made by comigration with authentic standards (Boggs et al., 1995a). Quantitation was done by scraping into liquid scintillation vials the silica gel from regions corresponding to migration of the standards.

Results

C_2-ceramide has been described to induce programmed cell death in many cell types (Hannun, 1996; Hartfield et al., 1997) including neuronal cells (Centeno et al., 1998; Tavarini et al., 2000; Willaime et al., 2001). Accordingly, we found that a 20-h exposure to C_2-ceramide decreased NB16 neuroblastoma cell viability in a dose-dependent manner (Fig. 1), with a half-maximally effective concentration of about 15 μM and 26.7 ± 9.9% cell survival after treatment with 20 μM C_2-ceramide. Treatment with 20 μM C_2-ceramide for 20 h triggered about 75% cell death overall (Fig. 1), but only 25% of the cells had TUNEL-positive nuclei (Fig. 2) after treatment with 20 μM C_2-ceramide, indicating DNA fragmentation characteristic of apoptosis. These data suggested that cell death was taking place through both apoptotic and nonapoptotic mechanisms. Exogenous synthetic ceramides with longer *N*-linked carbon chains were less toxic than C_2-ceramide (Ramos et al., 2002). The purpose of this investigation was to characterize the manner of cell death in response to exogenous ceramide treatment, thus we used the most potent analog (i.e., C_2-ceramide).

Ultrastructural analysis of NB16 neuroblastoma cells treated with 20 μM C_2-ceramide also revealed separate populations of cells with apoptotic and nonapoptotic morphological features (Fig. 3). Most cells were swollen, presenting a highly deteriorated cytoplasmic organization, with massive vacuolization (Fig. 3, B–G). We termed these cells "necrotic"; the necrotic cells were found as early as 2 h after C_2-ceramide addition. However, a subpopulation of cells had clear perinuclear chromatin condensation, indicative of apoptosis (Fig. 3, H–K). Those cells exhibiting chromatin condensation also displayed some extent of cytoplasmic vacuolization (Fig. 3, H–K), began to appear in the population about 8 h after treatment, and were scored as "mixed apoptotic/necrotic". The mixed apoptotic/necrotic cells reached a high degree of chromatin condensation at 20 to 24 h after C_2-ceramide. The time course was repeated with 40 μM C_2-ceramide and, comparing the results with those obtained with 20 μM C_2-ceramide, the percentage of necrotic cells was higher at the early time points, with more mixed morphologies appearing midway through the time course (data not shown). The results suggested that both apoptotic and necrotic mechanisms were involved in the cell death triggered by C_2-ceramide. To quantify the development of the two processes in the cell population, we monitored by flow cytometry the occurrence of cells with exposed phosphatidylserine (PtdSer) on the outer leaflet of the plasma membrane as one of the hallmarks of early

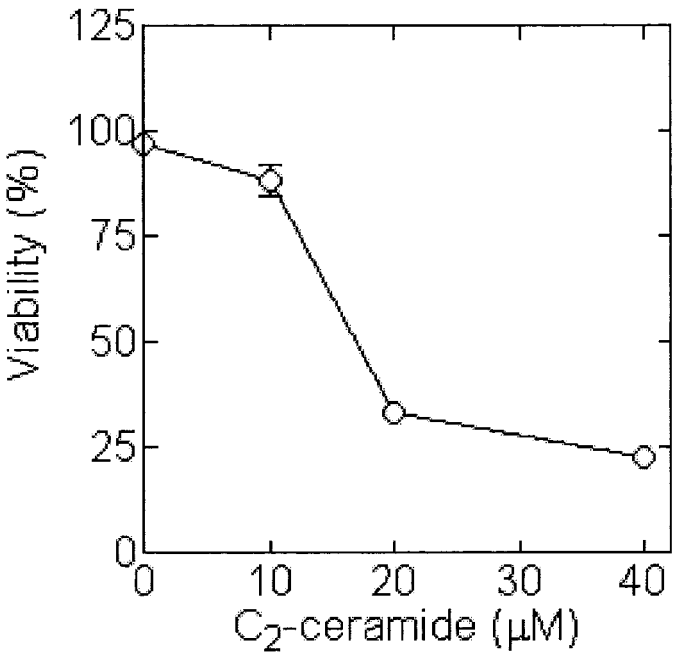

Fig. 1. C_2-ceramide reduces NB16 neuroblastoma cell viability. Cells were treated with the indicated C_2-ceramide concentrations for 20 h. Viability was determined by trypan blue exclusion as described under *Materials and Methods*. At least 100 cells were counted for each determination. Data represent the means ± range of a representative experiment. The experiment was performed three times with similar results.

apoptosis, together with cells permeable to PI because of loss of plasma membrane integrity, indicative of late apoptosis or necrosis (Vermes et al., 2000). It is likely that cells with mixed morphologies would be scored as apoptotic until the degree of vacuolization was great enough to destroy membrane integrity, thus permitting entry of the propidium iodide. The NB16 cells were also treated with TNFα + CHX as a positive control for apoptotis because these conditions have been characterized previously (Teitz et al., 2002). After short-term treatment (2, 4, and 8 h), TNFα + CHX induced a rapid increment in the number of cells with typical early apoptotic traits, exposing PtdSer to the outer leaflet (annexin V positive) while maintaining membrane integrity (PI-negative) (Fig. 4, B and E). The appearance of early apoptotic cells induced by TNFα + CHX peaked at 8 h (Table 1), and the early apoptotic population progressed to the late apoptotic phase thereafter. In contrast, the increase of annexin V-positive/PI-negative cells (early apoptotic) was barely manifested during the first 4 h of treatment with 20 μM C_2-ceramide (Fig. 4, C and E) but increased steadily up to 20 h. As shown in Table 1, the quantification of healthy cells (annexin V-negative/PI-negative), early apoptotic (annexin V-positive/PI-negative), and necrotic or late apoptotic (annexin V-positive/PI-positive) cells revealed that C_2-ceramide induced an increase of just 4.1% in early apoptotic cells, whereas TNFα + CHX triggered a 29.7% increase after 8 h of treatment. These results suggested that C_2-ceramide-induced apoptosis, measured as annexin V binding, progressed at a slower pace than that induced by TNFα + CHX. However, the analysis revealed that late apoptotic and/or necrotic cells, with disrupted plasma membrane integrity (annexin V-positive/PI-positive), increased steadily up to 20 h during both TNFα + CHX and C_2-ceramide treatments, reaching an occurrence of ~40% in both cases (Fig. 4F). Recalling that the percentage occurrence of early apoptotic cells after TNFα treatment decreased after 8 h, the data indicated a stepwise progression from early to late apoptosis in the case of TNFα + CHX. However, these results were also consistent with C_2-ceramide inducing the majority of cells to directly progress from healthy to late apoptotic (or rather, mixed or necrotic) status, whereas a minority of cells followed the transition through the early apoptotic appearance to late apoptosis.

As expected for an apoptotic process, we found that both

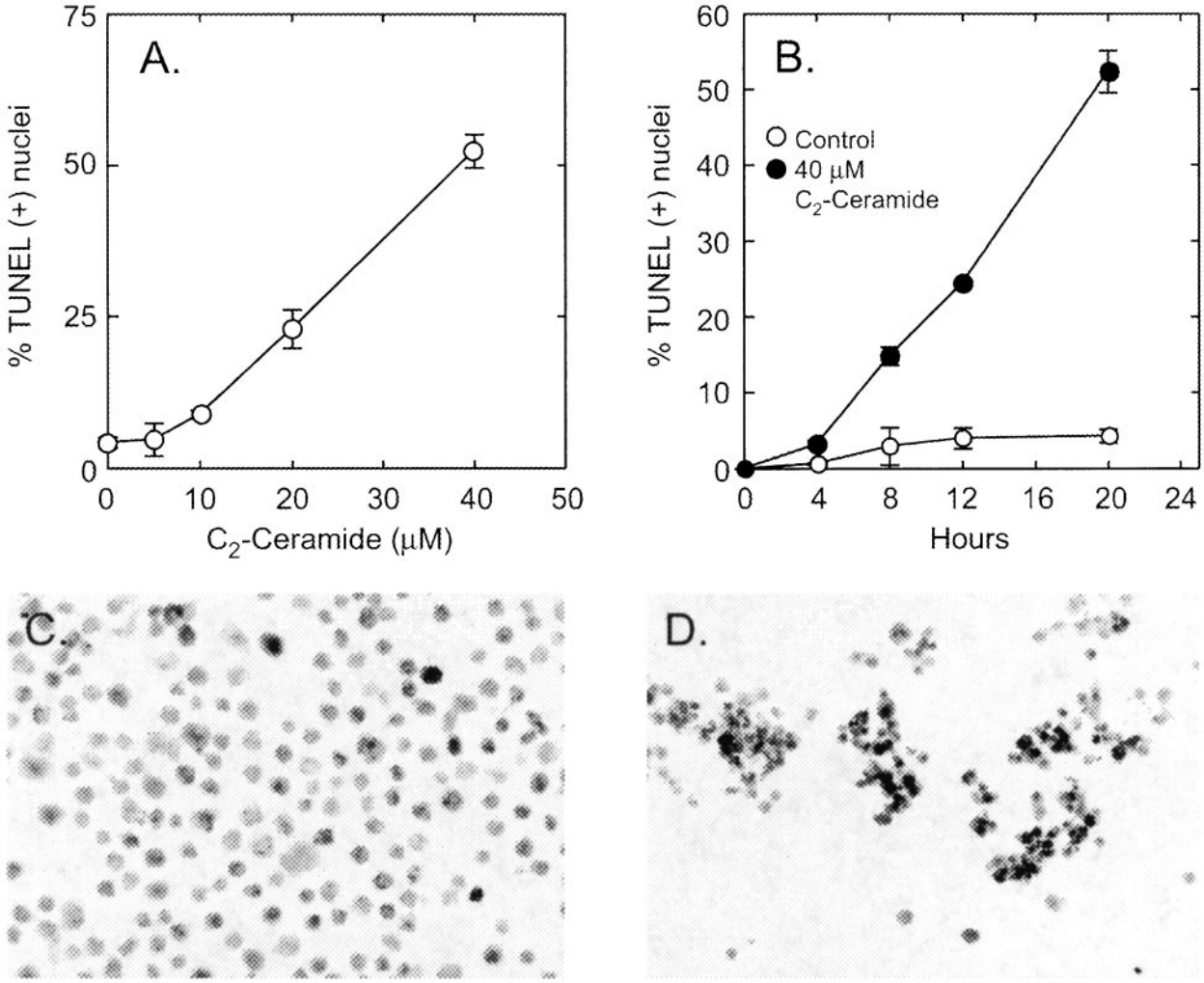

Fig. 2. C_2-ceramide induces DNA degradation. A, cells were treated with the indicated C_2-ceramide concentrations for 20 h. B, cells were treated for the indicated times with 40 μM C_2-ceramide. Occurrence of apoptosis was quantified by counting TUNEL-positive nuclei (or clusters of apoptotic bodies), and values were expressed relative to total nuclei. At least 100 nuclei were counted in each field and values are means ± S.D. from three experiments. Examples of in situ labeling of DNA fragmentation are shown after 20-h incubation under control conditions (C) or with 20 μM C_2-ceramide (D).

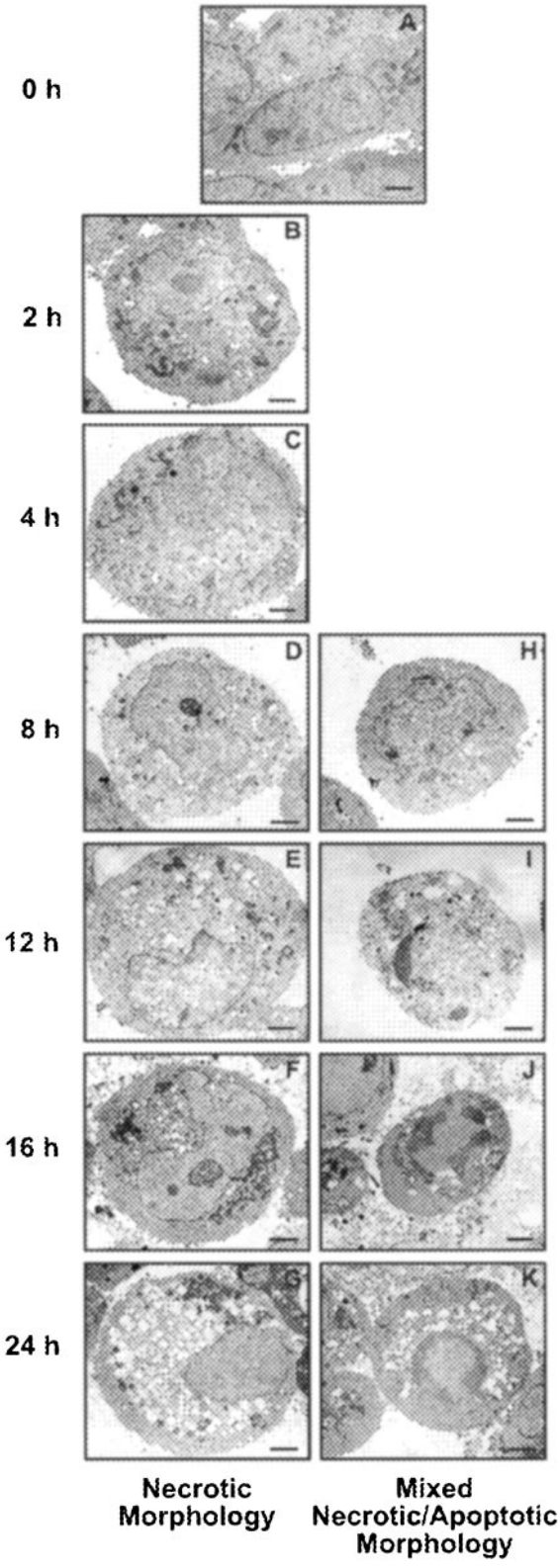

Fig. 3. Cells exposed to C_2-ceramide exhibit necrotic and apoptotic morphological alterations. Cells were incubated for times up to 24 h in 20 μM C_2-ceramide. A, control untreated cells; B to G, cells with necrotic ultrastructural alterations; H to K, cells with mixed necrotic and apoptotic characteristics at 2 (B), 4 (C), 8 (D and H), 12 (E and I), 16 (F and J), and 24 (G and K) h of C_2-ceramide treatment. Cells were fixed, stained, and viewed using electron microscopy as described under *Materials and Methods*. Scale bar, 2 μm. All images are shown at the same magnification.

caspase 8 and 3 activities were elevated in cytosolic extracts from cells exposed to C_2-ceramide or TNFα + CHX (Fig. 5, A and B). Caspase 8 peaked after 8 h of treatment both with TNFα + CHX or C_2-ceramide, reaching a slightly lower activity under C_2-ceramide treatment (Fig. 5A). Caspase 3 activation, on the other hand, was delayed 2 h for C_2-ceramide compared with TNFα-treated cells, although both treatments induced the same peak activity (Fig. 5B). Pretreatment of cells with the broad-spectrum caspase inhibitor z-VAD-fmk precluded the activation of caspases 8 (Fig. 5C) and 3 (Fig. 5D) by C_2-ceramide or TNFα + CHX. Interestingly, z-VAD-fmk was not able to prevent C_2-ceramide–triggered cell death but was fully effective against cells incubated with TNFα + CHX (Fig. 6A). Further analysis using flow cytometry of the cell distribution after labeling with annexin V and propidium iodide revealed that z-VAD-fmk prevented the appearance of early apoptotic cells after either C_2-ceramide or TNFα + CHX treatment (Fig. 6B). Addition of z-VAD-fmk caused a redistribution of cells into the healthy population after treatment with TNFα + CHX, whereas the caspase inhibitor caused redistribution into the necrotic population after C_2-ceramide treatment (Fig. 6B). Taken together, these results show that the specific blockage of the apoptotic pathway in a minority of C_2-ceramide-treated cells does not prevent cell death (Fig. 6A), although cell death induced by C_2-ceramide in NB16 cells takes place with concomitant activation of caspases. Rather, these activities are not required to initiate nor do they support the development of the predominant cell death mechanism induced by C_2-ceramide.

These results indicated that the cell death mediated by C_2-ceramide occurred by a caspase-independent mechanism. As an alternative explanation, C_2-ceramide was recently shown to directly inhibit the CTP:phosphocholine cytidylyltransferase step in PtdCho biosynthesis in COS-7 cells, and prior research has linked the inhibition of PtdCho biosynthesis to cytotoxicity caused by a variety of agents (Ramos et al., 2002, and references therein). We measured PtdCho biosynthesis in the NB16 cells treated with a range of C_2-ceramide concentrations up to 40 μM C_2-ceramide by radiolabeling cells for 4 h and found that PtdCho production was substantially reduced within this short time frame (Fig. 7). To investigate the reduction in PtdCho biosynthesis in more detail, we increased the amount of [*methyl*-^{3}H]choline added to the medium and conducted a time course experiment after addition of 40 μM C_2-ceramide. The inhibition of PtdCho formation was immediate and was accompanied by selective accumulation of phosphocholine (Fig. 8A), a metabolic precursor of PtdCho and the substrate for the cytidylyltransferase. These results are consistent with in vivo inhibition of the cytidylyltransferase and provide a reasonable mechanism for the cytotoxicity induced by C_2-ceramide. Taken together, the data also suggest that inhibition of PtdCho biosynthesis can lead to caspase activation and that cells may respond to reduced PtdCho production with multiple cell death processes rather than apoptosis exclusively.

Discussion

The present work defines the pathways for C_2-ceramide-mediated cytotoxicity by examining the morphological and biochemical traits of NB16 neuroblastoma cells exposed to C_2-ceramide. Cell swelling and extensive cytoplasmic vacu-

olization with minimal nuclear alteration is the most prominent ultrastructural feature of C_2-ceramide-treated cells. This is a characteristic feature of necrotic neuronal death (Ishitani et al., 1997; Fujikawa et al., 1999), although it also appears in some forms of nonapoptotic programmed cell death, as shown in cells treated with insulin-like growth factor I (Sperandio et al., 2000). A minor population of C_2-ceramide–treated cells displays clear perinuclear chromatin condensation together with cytosolic vacuolization, suggesting the simultaneous occurrence of necrosis and apoptosis in a minor population of cells. The generation of DNA strand breaks is a hallmark of apoptosis (Gavrieli et al., 1992), and comparison of cell viability after a 20-h exposure to 20 μM C_2-ceramide with the incidence of TUNEL-positive nuclei leads to the conclusion that approximately one third of the overall cytotoxicity is attributable to apoptosis. Early redistribution of PtdSer in the plasma membrane is a universal marker for apoptosis regardless of the initiating stimulus (Martin et al., 1995); therefore, the use of annexin V in combination with PI staining discriminates between apoptotic and necrotic cells (Vermes et al., 2000). The appearance of PtdSer in the outer leaflet of the plasma membrane is an early event in TNFα + CHX-treated cells. However, in the majority of C_2-ceramide–treated cells, annexin V accesses PtdSer-rich membranes when the cells become permeable to PI (Fig. 4E), revealing the necrotic-like disorganization of the plasma membrane. Again, a subset of C_2-ceramide–treated cells followed a typical apoptotic pattern of PtdSer exposure while maintaining membrane integrity. As expected, apoptosis induced by TNFα + CHX was dependent on caspase activity. Initiator caspase 8 and executor caspase 3 also became activated in C_2-ceramide-treated cells, again indicative of apoptosis. However, in this case, caspase blockade did not increase cell survival at all. This observation is in agreement with the simultaneous occurrence of necrotic and apoptotic events in at least a subset of cells and demonstrates that the apoptotic machinery is not the primary determinant of C_2-ceramide cytotoxicity. The fact that the inhibition of the apoptotic pathway increases the number of necrotic cells (Fig. 6B) demonstrates that C_2-ceramide activates necrotic

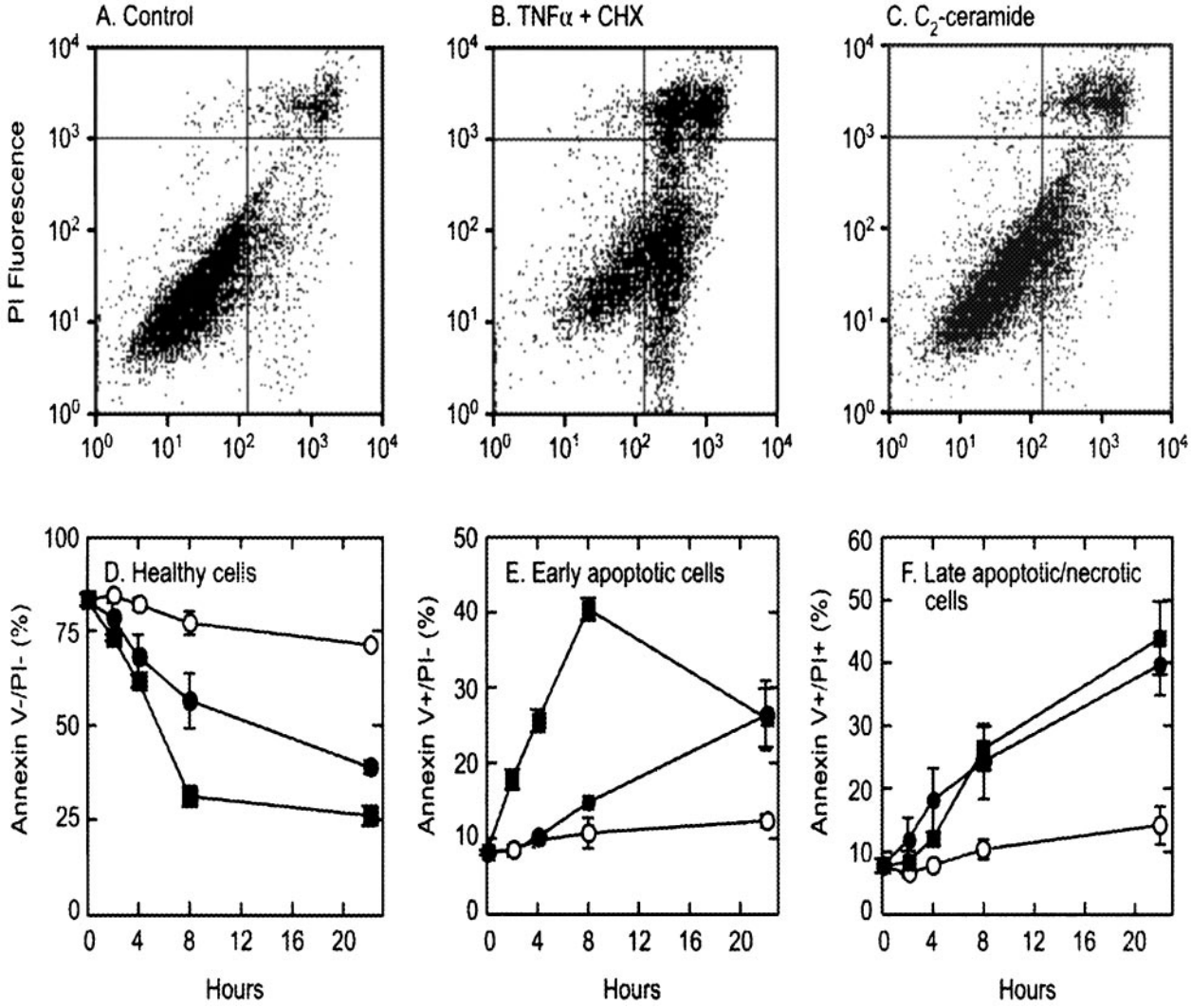

Fig. 4. C_2-ceramide-treated cells display a necrotic pattern of annexin V and PI labeling. Cells were maintained under control conditions (A) or treated with TNFα (100 ng/ml) plus cycloheximide (20 μg/ml) (B) or 20 μM C_2-ceramide (C) for 8 h. D to F, cells were treated with 20 μM C_2-ceramide (●), TNFα (100 ng/ml) plus cycloheximide (20 μg/ml) (■), or DMSO plus ethanol vehicle (○) for the indicated times up to 22 h. Annexin V, propidium iodide staining, and flow cytometric analysis were performed as described under *Materials and Methods*. Data in D to F are means ± S.D. of duplicate determinations from three experiments

TABLE 1

Quantification of annexin V binding and propidium iodide permeability in cells treated with C_2-ceramide or TNFα for 8 h

Cells were treated with 20 μM C_2-ceramide, TNFα (100 ng/ml) plus cycloheximide (20 μg/ml), or DMSO plus ethanol vehicle controls for 8 h. Cells were stained with annexin V and propidium iodide and analyzed by flow cytometry as described under *Materials and Methods*. Healthy cells were annexin V-negative/PI-negative. Early apoptotic cells were annexin V-positive/PI-negative. Necrotic cells were annexin V-positive/PI-positive. Data are expressed as percentage occurrence of each cell population in each sample and are means ± S.D. of duplicate determinations from three experiments.

	Control	TNFα + CHX	C_2-Ceramide
Healthy cells	77.0 ± 3.1	31.1 ± 2.6	56.4 ± 7.2
Early apoptotic cells	10.7 ± 2.0	40.4 ± 1.5	14.8 ± 0.9
Late apoptotic/necrotic cells	10.3 ± 1.6	26.3 ± 3.5	24.3 ± 5.9

mechanisms in virtually all of the cells. Thus, based on ultrastructural and biochemical criteria, including the appearance of DNA strand breaks and loss of phospholipid asymmetric distribution, our results show consistently the prevalence of necrotic over apoptotic cell death induced by C_2-ceramide.

C_2-ceramide cytotoxicity in neuroblastoma (Ito et al., 1999) and oligodendroglial (Craighead et al., 2000) cell lines has been reported to take place with cell shrinkage, chromatin condensation, DNA fragmentation, and caspase activation, supporting apoptosis as a mechanism for cell death. Furthermore, treatment with caspase inhibitors prevents DNA fragmentation (Ito et al., 1999) or the development of apoptotic morphology (Craighead et al., 2000). These reports are not in conflict with ours. Our studies also show that an apoptotic mechanism operates in the C_2-ceramide-treated cell population. However, these previous reports made no attempt to assess cell viability after caspase inhibition and may have overlooked the necrotic cell death. In support of our conclusions, there is evidence to suggest that C_2-ceramide may induce both apoptotic and nonapoptotic mechanisms of cell death working in parallel. PC12 cells undergo apoptosis after

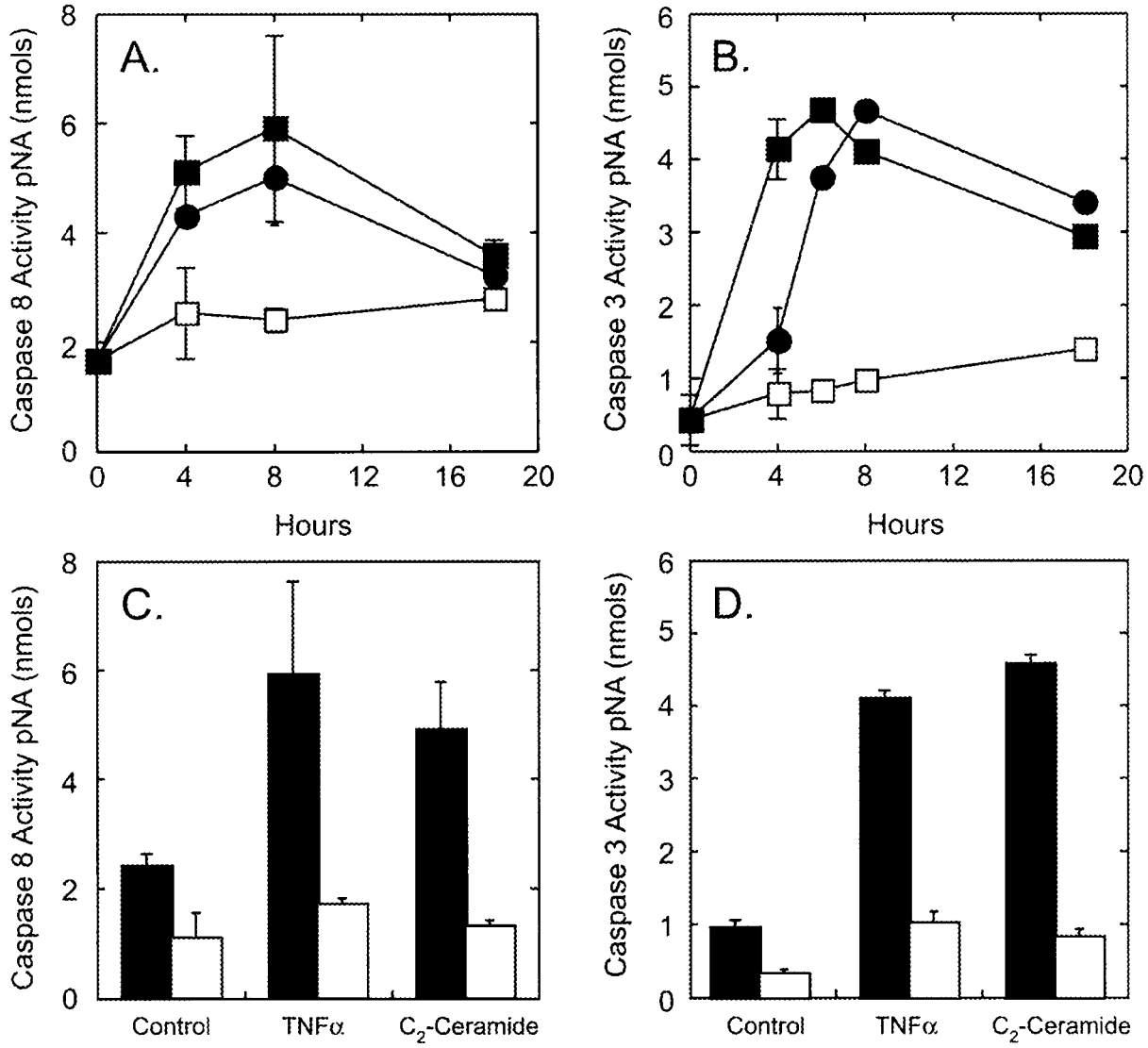

Fig. 5. C_2-ceramide activates caspase-8 and caspase-3. Cells were treated with 20 μM C_2-ceramide (●), TNFα (100 ng/ml) plus cycloheximide (20 μg/ml) (■), or DMSO plus ethanol vehicles (○) for the indicated times (A and B) or 8 h (C and D). One hour before treatment, cells were incubated with 80 μM z-VAD-fmk (■) or DMSO (□) (C and D). A and C, caspase-8–like activity was measured in cell lysates using IETD-*p*-nitroanilide (pNA) substrate as described under *Materials and Methods*. B and D, caspase-3–like activity was measured in cell lysates using DEVD-pNA as substrate. The data are means ± range of duplicate samples in a representative experiment.

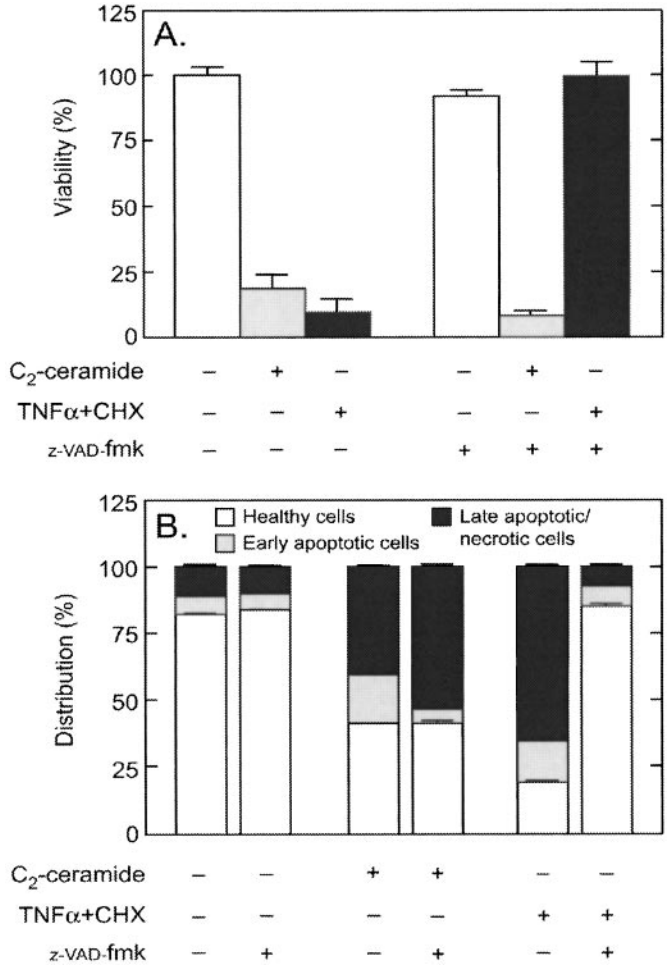

Fig. 6. Caspase inhibition does not prevent cell death induced by C_2-ceramide. Cells were incubated with 80 μM z-VAD-fmk for 1 h, then treated with 20 μM C_2-ceramide, TNFα (100 ng/ml) plus cycloheximide (20 μg/ml), or vehicle controls for 20 h. A, mean viable cells ± S.D. of duplicate determinations from three independent experiments as determined by trypan blue exclusion. Total cell number for control was 4.14×10^5; C_2-ceramide, 4.26×10^5; TNFα + CHX, 4.90×10^5; z-VAD-fmk, 6.34×10^5; C_2-ceramide + z-VAD-fmk, 6.05×10^5; TNFα + CHX + z-VAD-fmk, 4.08×10^5. B, distribution of cells scored as healthy (annexin V−/PI−); early apoptotic (annexin V+/PI−); late apoptotic or necrotic (annexin V+/PI+). Data are expressed as percentage occurrence of each cell population in each sample and are means ± S.D. of duplicate determinations from three experiments.

exposure to C_2-ceramide, but caspase inhibitors are unable to prevent cell death (Hartfield et al., 1997). Also, cerebellar granule cells undergo apoptosis-like changes, such as formation of DNA nicks and internucleosomal fragmentation; again, however, treatment with caspase inhibitors is unable to rescue neurons (Monti et al., 2001). Our work provides strong support for the simultaneous occurrence of necrosis and apoptosis after C_2-ceramide treatment and challenges the reliability of using short-chain analogs of ceramide to reproduce the biological effects of endogenous ceramide that have been reported to accompany challenge with physiological apoptotic stimuli, such as TNFα. Reports about the lack of caspase activation during C_2-ceramide–mediated apoptosis suggest that the apoptotic process might be mediated by calpain or other proteases (Belaud-Rotureau et al., 1999; Poppe et al., 2002). These findings open the possibility that a subset of dying NB16 neuroblastoma cells arise from proteolytic activities other than caspases.

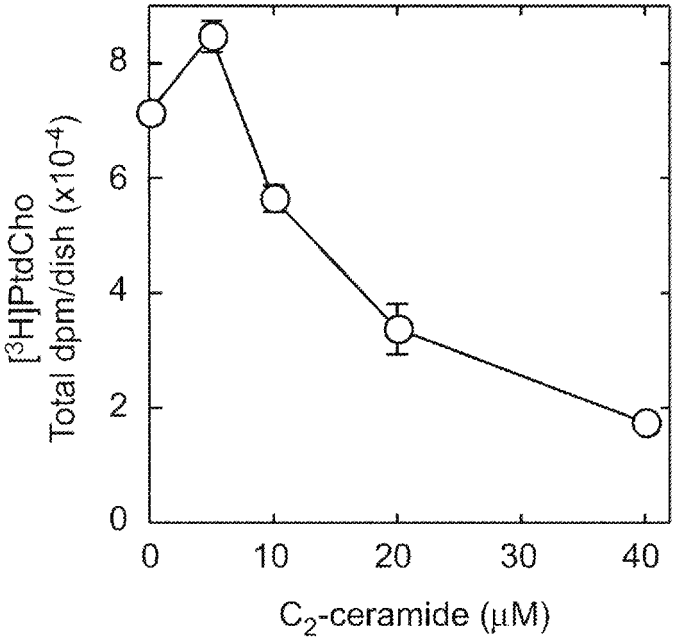

Fig. 7. C_2-ceramide inhibits PtdCho biosynthesis in a dose-dependent manner. Cells were incubated with the indicated concentration of C_2-ceramide and [*methyl*-^{3}H]choline (2 μCi/ml) for 4 h. Cells were harvested and lipids were quantified as described under *Materials and Methods*. Total radioactivity incorporated into the lipid fraction was ≥95% PtdCho. The data are the means ± range from duplicates in a representative experiment.

Although short-chain analogs mimic many biological effects of ceramide-mediated signaling of death receptors (Hannun, 1996), our results and those of Belaud-Rotureau et al. (1999) illustrate that the key targets accounting for the cytotoxicity of C_2-ceramide must be different from those of endogenous ceramide after TNFα or Fas ligand binding. We have demonstrated recently that CTP:phosphocholine cytidylyltransferase, the key enzyme in the biosynthesis of PtdCho, is directly inhibited by C_2-ceramide, whereas long-chain ceramide did not inhibit this enzyme (Ramos et al., 2002). This inhibitory effect is very similar to that of ET-18-OCH_3 and other alkylphosphocholines (Boggs et al., 1995a,b; Ramos et al., 2002) used as anticancer drugs. It has been reported recently that the antitumoral drug erucylphosphocholine exerts an apoptotic effect on glioma cells, including the processing of procaspases-3, -7, -8, and -9 into the active forms; interestingly, caspase inhibitors prevented apoptosis but did not abrogate cell death (Kugler et al., 2002), providing evidence for the existence of a caspase-independent pathway turned on by this drug. In the search for the molecular basis of the cytotoxicity of erucylphosphocholine, these authors demonstrate the lack of involvement of the TNF or TNF-related ligand apoptotic pathways. Erucylphosphocholine, just like other alkylphosphocholines, is likely to be an inhibitor of CTP:phosphocholine cytidylyltransferase as effective as C_2-ceramide or ET-18-OCH_3, and inactivation of this target could account for the strikingly similar cytotoxic profiles of these molecules. Caspase-independent cytotoxicity may be a general feature of inhibitors of PtdCho biosynthesis. This constitutes a promising strategy for the development of antitumoral drugs, because tumor cells often have defective caspase-dependent pathways. In many neuroblastomas, the gene for caspase 8 is silenced, rendering these tumors resis-

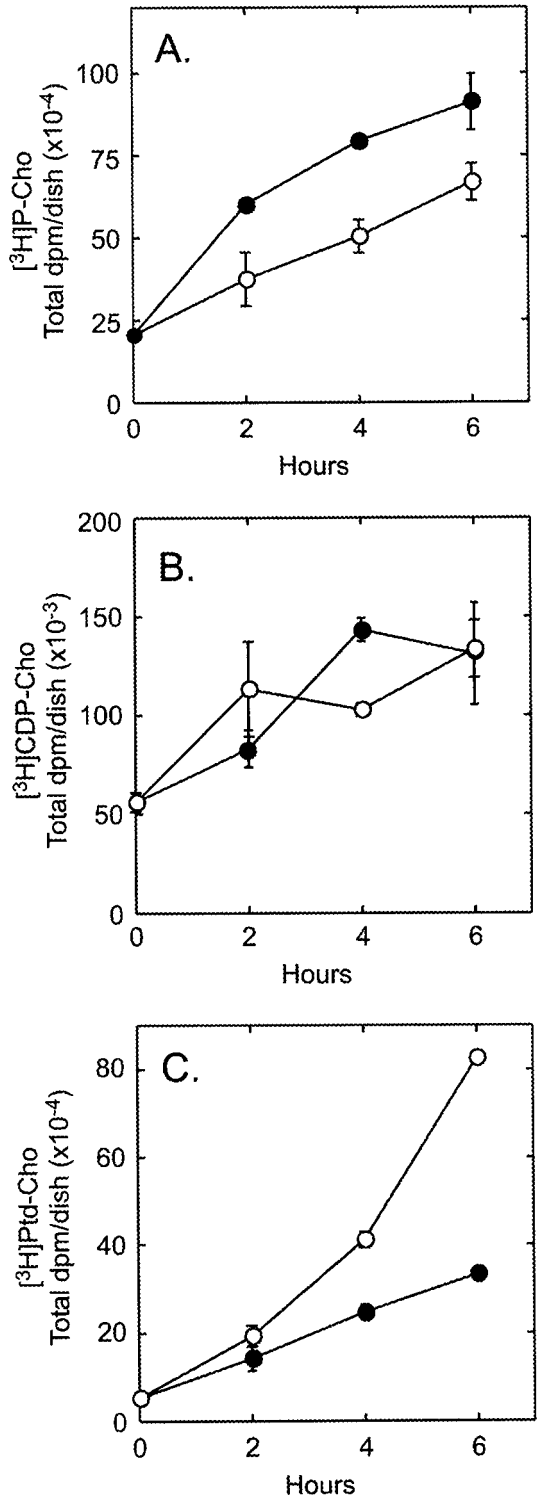

Fig. 8. C_2-ceramide inhibits PtdCho biosynthesis at the CTP:phosphocholine cytidylyltransferase step. Cells were labeled with [*methyl*-^{3}H]choline (10 μCi/ml) for 2 h and incubation continued in the absence (○) or presence (●) of 40 μM C_2-ceramide for the times indicated. Cells were harvested and lipids were extracted as described under *Materials and Methods*. Total radioactivity incorporated into [^{3}H]lipid organic fraction, representing ≥95% PtdCho, was detected by liquid scintillation counting (C). The aqueous precursor [^{3}H]metabolites were separated by thin-layer chromatography as described under *Materials and Methods* and the radioactivity comigrating with authentic choline, phosphocholine (A), and cytidinediphosphocholine (B) was detected by liquid scintillation counting. The data are the means ± range from duplicates in a representative experiment and the experiment was repeated three times with similar results.

tant to death receptor- and doxorubucin-mediated apoptosis (Teitz et al., 2000, 2002).

The fact that C_2-ceramide targets PtdCho synthesis at the cytidylyltransferase step (Ramos et al., 2002) suggests that other agents that kill cells by blocking PtdCho production may also trigger two different pathways leading to cell death. Previous investigators, including us, may have overlooked the possibility that necrotic cell death may have accompanied apoptotic cell death because of the limitations of the assays and lack of consideration of alternative death mechanisms.

Acknowledgments

We thank M. El Mouedden for the TUNEL assays; Dr. Gopal Murti, SJCRH Scientific Imaging Shared Resource, for the electron micrographs; and Dr. Richard Ashmun, SJCRH Flow Cytometry Shared Resource, for the fluorescence-activated cell sorting analysis of cells stained with annexin V and propidium iodide. We also thank Dr. Charles O. Rock for helpful discussion and comments on the manuscript and Daren Hemingway for excellent technical assistance.

References

Allan D (2000) Lipid metabolic changes caused by short-chain ceramides and the connection with apoptosis. *Biochem J* **345:**603–610.

Anthony ML, Zhao M, and Brindle KM (1999) Inhibition of phosphatidylcholine biosynthesis following induction of apoptosis in HL-60 cells. *J Biol Chem* **274:** 19686–19692.

Ashkenazi A and Dixit VM (1998) Death receptors: signaling and modulation. *Science (Wash DC)* **281:**1305–1308.

Baburina I and Jackowski S (1998) Apoptosis triggered by 1-*O*-octadecyl-2-*O*-methyl-*rac*-glycero-3-phosphocholine is prevented by increased expression of CTP: phosphocholine cytidylyltransferase. *J Biol Chem* **273:**2169–2173.

Belaud-Rotureau MA, Lacombe F, Durrieu F, Vial JP, Lacoste L, Bernard P, and Belloc F (1999) Ceramide-induced apoptosis occurs independently of caspases and is decreased by leupeptin. *Cell Death Differ* **6:**788–795.

Bligh EG and Dyer WJ (1959) A rapid method of total lipid extraction and purification. *Can J Biochem Physiol* **37:**911–917.

Boggs KP, Rock CO, and Jackowski S (1995a) Lysophosphatidylcholine and 1-*O*-octadecyl-2-*O*-methyl-*rac*-glycero-3-phosphocholine inhibit the CDP-choline pathway of phosphatidylcholine synthesis at the CTP:phosphocholine cytidylyltransferase step. *J Biol Chem* **270:**7757–7764.

Boggs KP, Rock CO, and Jackowski S (1995b) Lysophosphatidylcholine attenuates the cytotoxic effects of the antineoplastic phospholipid 1-*O*-octadecyl-2-*O*-methyl-*rac*-glycero-3-phosphocholine. *J Biol Chem* **270:**11612–11618.

Bose R, Verheij M, Haimovitz-Friedman A, Scotto K, Fuks Z, and Kolesnick R (1995) Ceramide synthase mediates daunorubicin-induced apoptosis: an alternative mechanism for generating death signals. *Cell* **82:**405–414.

Centeno F, Mora A, Fuentes JM, Soler G, and Claro E (1998) Partial lithium-associated protection against apoptosis induced by C_2-ceramide in cerebellar granule neurons. *Neuroreport* **9:**4199–4203.

Clarke PG (1990) Developmental cell death: morphological diversity and multiple mechanisms. *Anat Embryol (Berl)* **181:**195–213.

Craighead M, Pole J, and Waters C (2000) Caspases mediate C_2-ceramide-induced apoptosis of the human oligodendroglial cell line, M03.13. *Neurosci Lett* **278:**125–128.

Dal Canto MC and Gurney ME (1994) Development of central nervous system pathology in a murine transgenic model of human amyotrophic lateral sclerosis. *Am J Pathol* **145:**1271–1279.

El Mouedden M, Laurent G, Mingeot-Leclercq MP, and Tulkens PM (2000) Gentamicin-induced apoptosis in renal cell lines and embryonic rat fibroblasts. *Toxicol Sci* **56:**229–239.

Fujikawa DG, Shinmei SS, and Cai B (1999) Lithium-pilocarpine-induced status epilepticus produces necrotic neurons with internucleosomal DNA fragmentation in adult rats. *Eur J Neurosci* **11:**1605–1614.

Gavrieli Y, Sherman Y, and Ben Sasson SA (1992) Identification of programmed cell death in situ via specific labeling of nuclear DNA fragmentation. *J Cell Biol* **119:**493–501.

Genestier L, Prigent AF, Paillot R, Quemeneur L, Durand I, Banchereau J, Revillard JP, and Bonnefoy-Berard N (1998) Caspase-dependent ceramide production in Fas- and HLA class I-mediated peripheral T cell apoptosis. *J Biol Chem* **273:**5060–5066.

Hannun YA (1996) Functions of ceramide in coordinating cellular responses to stress. *Science (Wash DC)* **274:**1855–1859.

Hannun YA and Luberto C (2000) Ceramide in the eukaryotic stress response. *Trends Cell Biol* **10:**73–80.

Hartfield PJ, Mayne GC, and Murray AW (1997) Ceramide induces apoptosis in PC12 cells. *FEBS Lett* **401:**148–152.

Haug JS, Goldner CM, Yazlovitskaya EM, Voziyan PA, and Melnykovych G (1994) Directed cell killing (apoptosis) in human lymphoblastoid cells incubated in the presence of farnesol: effect of phosphatidylcholine. *Biochim Biophys Acta* **1223:** 133–140.

Ishitani R, Sunaga K, Tanaka M, Aishita H, and Chuang DM (1997) Overexpression of glyceraldehyde-3-phosphate dehydrogenase is involved in low K^+-induced apoptosis but not necrosis of cultured cerebellar granule cells. *Mol Pharmacol* **51:**542–550.

Ito A, Uehara T, Tokumitsu A, Okuma Y, and Nomura Y (1999) Possible involvement of cytochrome c release and sequential activation of caspases in ceramide-induced apoptosis in SK-N-MC cells. *Biochim Biophys Acta* **1452:**263–274.

Kerr JF, Wyllie AH, and Currie AR (1972) Apoptosis: a basic biological phenomenon with wide-ranging implications in tissue kinetics. *Br J Cancer* **26:**239–257.

Kugler W, Erdlenbruch B, Junemann A, Heinemann D, Eibl H, and Lakomek M (2002) Erucylphosphocholine-induced apoptosis in glioma cells: involvement of death receptor signalling and caspase activation. *J Neurochem* **82:**1160–1170.

Leist M and Jäättelä M (2001) Four deaths and a funeral: from caspases to alternative mechanisms. *Nat Rev Mol Cell Biol* **2:**1–10.

Lipton SA and Nicotera P (1998) Calcium, free radicals and excitotoxins in neuronal apoptosis. *Cell Calcium* **23:**165–171.

Majno G and Joris I (1995) Apoptosis, oncosis and necrosis. An overview of cell death. *Am J Pathol* **146:**3–15.

Martin SJ, Reutelingsperger CP, McGahon AJ, Rader JA, van Schie RC, LaFace DM, and Green DR (1995) Early redistribution of plasma membrane phosphatidylserine is a general feature of apoptosis regardless of the initiating stimulus: inhibition by overexpression of Bcl-2 and Abl. *J Exp Med* **182:**1545–1556.

Mathias S, Pena LA, and Kolesnick RN (1998) Signal transduction of stress via ceramide. *Biochem J* **335:**465–480.

Miquel K, Pradines A, Terce F, Selmi S, and Favre G (1998) Competitive inhibition of choline phosphotransferase by geranylgeraniol and farnesol inhibits phosphatidylcholine synthesis and induces apoptosis in human lung adenocarcinoma A549 cells. *J Biol Chem* **273:**26179–26186.

Monti B, Zanghellini P, and Contestabile A (2001) Characterization of ceramide-induced apoptotic death in cerebellar granule cells in culture. *Neurochem Int* **39:**11–18.

Poppe M, Reimertz C, Munstermann G, Kogel D, and Prehn JH (2002) Ceramide-induced apoptosis of D283 medulloblastoma cells requires mitochondrial respiratory chain activity but occurs independently of caspases and is not sensitive to Bcl-xL overexpression. *J Neurochem* **82:**482–494.

Ramos B, El Mouedden M, Claro E, and Jackowski S (2002) Inhibition of CTP: phosphocholine cytidylyltransferase by C_2-ceramide and its relationship to apoptosis. *Mol Pharmacol* **62:**1068–1075.

Ramos B, Salido GM, Campo ML, and Claro E (2000) Inhibition of phosphatidylcholine synthesis precedes apoptosis induced by C_2-ceramide: protection by exogenous phosphatidylcholine. *Neuroreport* **11:**1–6.

Rodriguez-Lafrasse C, Alphonse G, Aloy MT, Ardail D, Gerard JP, Louisot P, and Rousson R (2002) Increasing endogenous ceramide using inhibitors of sphingolipid metabolism maximizes ionizing radiation-induced mitochondrial injury and apoptotic cell killing. *Int J Cancer* **101:**589–598.

Sperandio S, de B, I and Bredesen DE (2000) An alternative, nonapoptotic form of programmed cell death. *Proc Natl Acad Sci USA* **97:**14376–14381.

Tavarini S, Colombaioni L, and Garcia-Gil M (2000) Sphingomyelinase metabolites control survival and apoptotic death in SH-SY5Y neuroblastoma cells. *Neurosci Lett* **285:**185–188.

Teitz T, Wei T, Liu D, Valentine V, Valentine M, Grenet J, Lahti JM, and Kidd VJ (2002) Caspase-9 and Apaf-1 are expressed and functionally active in human neuroblastoma tumor cell lines with 1p36 LOH and amplified MYCN. *Oncogene* **21:**1848–1858.

Teitz T, Wei T, Valentine MB, Vanin EF, Grenet J, Valentine VA, Behm FG, Look AT, Lahti JM, and Kidd VJ (2000) Caspase 8 is deleted or silenced preferentially in childhood neuroblastomas with amplification of MYCN. *Nat Med* **6:**529–535.

Vermes I, Haanen C, and Reutelingsperger C (2000) Flow cytometry of apoptotic cell death. *J Immunol Methods* **243:**167–190.

Voziyan A, Goldner CM, and Melnykovych G (1993) Farnesol inhibits phosphatidylcholine biosynthesis in cultured cells by decreasing cholinephosphotransferase activity. *Biochem J* **295:**757–762.

Willaime S, Vanhoutte P, Caboche J, Lemaigre-Dubreuil Y, Mariani J, and Brugg B (2001) Ceramide-induced apoptosis in cortical neurons is mediated by an increase in p38 phosphorylation and not by the decrease in ERK phosphorylation. *Eur J Neurosci* **13:**2037–2046.

Address correspondence to: Dr. Suzanne Jackowski, Protein Science Division, Department of Infectious Diseases, St Jude Children's Research Hospital, 332 North Lauderdale St., Memphis, TN 38105-2794. E-mail: suzanne.jackowski@stjude.org